
Enzymology:


# Pre-Steady-State Kinetic and Structural Analysis of Interaction of Methionine γ -Lyase from Citrobacter freundii with Inhibitors

Nikita A. Kuznetsov, Nicolai G. Faleev, Alexandra A. Kuznetsova, Elena A. Morozova, Svetlana V. Revtovich, Natalya V. Anufrieva, Alexei D. Nikulin, Olga S. Fedorova and Tatyana V. Demidkina

*J. Biol. Chem.* published online November 14, 2014

JBC Papers in Press. Published on November 14, 2014 as Manuscript M114.586511
The latest version is at http://www.jbc.org/cgi/doi/10.1074/jbc.M114.586511


# Pre-Steady-State Kinetic and Structural Analysis of Interaction of Methionine γ-Lyase from *Citrobacter freundii* with Inhibitors*

**Nikita A. Kuznetsov[1,2], Nicolai G. Faleev[3], Alexandra A. Kuznetsova[1,2], Elena A. Morozova[4], Svetlana V. Revtovich[4], Natalya V. Anufrieva[4], Alexei D. Nikulin[5], Olga S. Fedorova[1,2,§], Tatyana V. Demidkina[4,§]**

[1]Institute of Chemical Biology and Fundamental Medicine, Siberian Branch of the Russian Academy of Sciences, Novosibirsk 630090, Russia
[2]Department of Natural Sciences, Novosibirsk State University, Novosibirsk 630090, Russia
[3]Nesmeyanov Institute of Organoelement Compounds, Russian Academy of Sciences, Moscow 119991, Russia
[4]Engelhardt Institute of Molecular Biology, Russian Academy of Sciences, Moscow 119991, Russia
[5]Institute of Protein Research, Russian Academy of Sciences, Pushchino, Moscow Region, 142290, Russia

*Running title: *Kinetic and Structural Studies of Inhibitors of Methionine γ-Lyase*

[§]To whom correspondence should be addressed: O.S.F. Tel: +7(383)363 5174, Email: fedorova@niboch.nsc.ru; T.V.D. Tel.: +7(499)135 9858, Email: tvd@eimb.ru

**Keywords:** Pyridoxal 5'-phosphate dependent methionine γ-lyase, competitive inhibitors, pre-steady-state kinetics, spatial structure of pyridoxal 5'-phosphate-cycloserine derivative.

**Background:** Speculative chemical mechanism of methionine γ-lyase is formulated, kinetic and structural data concerning elementary stages of physiological reaction are mostly lacking.
**Results:** Pre-steady-state kinetic and structural analysis of the enzyme interaction with inhibitors was performed.
**Conclusion:** Results elucidate mechanism of intermediates interconversion at initial stages of enzymatic reaction.
**Significance:** The data serve for understanding detailed mechanism of pyridoxal 5′-phosphate dependent γ-elimination reaction.

## ABSTRACT

**MGL catalyzes the γ-elimination of L-methionine and its derivatives as well as the β-elimination of L-cysteine and its analogs. These reactions yield α-keto acids and thiols. The mechanism of chemical conversion of amino acids includes numerous reaction intermediates. The detailed analysis of MGL interaction with glycine, L-alanine, L-norvaline and L-cycloserine was performed by pre-steady-state stopped-flow kinetics. The structure of side chains of the amino acids is important both for their binding with enzyme and for the stability of the external aldimine and ketimine intermediates. X-ray structure of MGL-L-cycloserine complex has been solved at 1.6 Å resolution. The structure models ketimine intermediate of physiological reaction. The results elucidate the mechanisms of the intermediates interconversion at the stages of external aldimine and ketimine formation.**

Methionine γ-lyase (EC 4.4.1.11, MGL), a pyridoxal 5'-phosphate (PLP) dependent enzyme, is found in many bacteria (1) including *Enterobacteriaceae* family (*Citrobacter freundii* (2)) and in pathogenic bacteria (*Bacteroides* ssp. (3), *Aeromonas* sp. (4), *Clostridium sporogenes* (5), *Porphyromonas gingivalis* (6), *Treponema denticola* (7)). MGL has also been found in parasitic eukaryotes (the protozoa *Entamoeba histolytica* (8) and *Trichomonas vaginalis* (9)) and in a plant *Arabidopsis thaliana* (10).

The absence of the enzyme in mammals allows MGL to be considered as a drug target for the treatment of infectious diseases. In addition, MGL has been utilized to develop the therapeutic treatment of tumors, by introducing recombinant proteins to deplete methionine, which is essential for the growth of cancer cells (11-13).

The biological unit of MGL is a tetramer which can be subdivided into two so-called catalytic dimers. Every dimer contains two active sites

consisting of amino acid residues from the both subunits and two molecules of PLP covalently bound to Lys210 (14).

MGL catalyzes the irreversible γ-elimination of L-methionine to give methanethiol, α-ketobutyrate and ammonia (Eq. 1). The enzyme is also able to catalyze β-elimination reaction of L-cysteine and S-substituted L-cysteines (Eq. 2) and γ- and β-replacement reactions of L-methionine and L-cysteine and their analogs (15,16). The chemical mechanism (Scheme 1) of γ-elimination reaction was proposed by Brzovic (17).

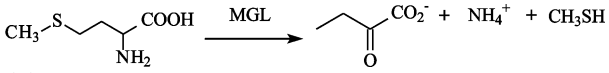


(1)

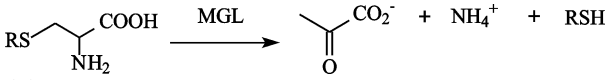


(2)

The initial stages of the γ-elimination occur by the exchange of ε-amino group of Lys210 in internal aldimine (I) to α-amino group of L-methionine through the fast formation of the geminal diamine (II) and its following conversion to the external aldimine (III). In the external aldimine (III) the proton is abstracted from the α-carbon atom of substrate and a quinonoid intermediate (IV) is formed. Subsequent protonation of the C4'-atom of the coenzyme and abstraction of a Cβ-proton of the substrate leads to the formation of ketimine (V) and enamine (VI) intermediates. The elimination of the thiol group, the sequential formation of β,γ-unsaturated ketimine (VII), α-aminocrotonate (VIII) and hydrolysis of the Schiff base in α-aminocrotonate lead finally to release of α-keto acid and ammonia. Intermediates of the γ-elimination reaction catalyzed by PLP-dependent enzymes possess the distinct absorption spectra (18).

Despite of spectral and structural information concerning MGL (14,19-21) the kinetic mechanisms of β- and γ-elimination reactions catalyzed by the enzyme remain poorly understood. Therefore, the detailed analysis of the changes in the absorption spectra accompanying the binding of the amino acids allows us to elucidate the mechanisms of the intermediates interconversion.

In the present work we have studied the kinetic mechanisms of binding of MGL from *C. freundii* with competitive inhibitors, glycine, L-alanine, L-norvaline and L-cycloserine. The stopped-flow kinetic analysis of the single-wavelength absorbance permitted us to attribute them separately to particular intermediates of the reaction. X-ray structure, modeling the ketimine intermediate of the γ-eliminating reaction, has been solved at 1.6 Å resolution. These data will serve for elucidation of mechanisms of physiological reaction catalyzed by *C. freundii* MGL and can be helpful for a design of new inhibitors of MGL as potential drugs for a treatment of infection diseases.

## EXPERIMENTAL PROCEDURES

*Materials, amino acids, enzymes* – All chemicals were from Sigma-Aldrich (St Louis, MO).

The recombinant MGL was obtained from *Escherichia coli* BL 21 (DE3) cells containing pET-mgl plasmid with the inserted *megL* gene from *C. freundii* genome. Growing of the cells and purification of the enzyme was carried out as described previously (2). Protein concentrations were determined by the method of Lowry *et al*. (22), using bovine serum albumin as a standard. Activity of the enzyme was assayed by measuring the rate of α-ketobutyrate formation from L-methionine by the method of Friedemann and Haugen (23). One unit of enzymic activity was determined as the amount of enzyme catalyzing transformation of 1 μmol of L-methionine per min at 30 °C. The specific activity of MGL was 8.5 u/mg.

*Pre-steady state stopped-flow studies* – Stopped-flow measurements with absorption detection were carried out using a model SX20 stopped-flow spectrometer (Applied Photophysics, U.K.) with a 150 W Xenon lamp and 10 mm pathlength optical cell. The dead time of the instrument was 1.0 ms. All experiments were carried out at 25 °C in 0.1 M potassium phosphate buffer solution (pH 7.8), containing 0.5 mM DTT and 0.1 mM EDTA. Solutions of enzyme (12.5 μM) were mixed with various concentrations of glycine (10-500 mM), L-alanine (1.0-12.0 mM), L-cycloserine (6.35-38.1 μM), and L-norvaline (1.5-7.5 mM). Each kinetic curve was averaged over at least three independent experiments. The absorbance at 320, 420 and 500 nm was detected.

*Kinetic data analysis* – Estimation of the kinetic mechanisms as well as the number of individual reaction steps was implemented as follows. Each kinetic trace was fitted by sum of

the exponential to define observed rate constants $k_{obs}$.

$$D_c = A1\times\exp(-k_{obs}^{1}\times t) + A2\times(1 - \exp(-k_{obs}^{2}\times t)) + D_b$$

$D_c$ is the absorbance intensity at any reaction time t; A1, A2 are the amplitudes; $k_{obs}^{1}$, $kobs^{2}$ are the observed rate constants; $D_b$ is the background absorbance.

Values of the observed rate constants $k_{obs}$ were plotted versus amino acid concentrations in order to estimate the individual rate constants. As an example the concentration dependence of $k_{obs}$ for the fast and slow phases at 320 nm for L-Ala are shown in Supplementary Figure S1. The fast phase fits a straight line according to the function $k_{obs}^{1} = k_1\times[\text{L-Ala}]+k_{-1}$. The slow phase fits the function $k_{obs}^{2} = K_b\times[\text{L-Ala}]\times k_2/(K_b\times[\text{L-Ala}]+1)+k_{-2}$. The dependences of $k_{obs}^{i}$ on L-Ala concentration allow to estimate all individual rate constants (Supplementary Figure S1), which were subsequently used as initial values in a global analysis.

Global non-linear least-squares fitting was performed using DynaFit4 software (BioKin Ltd) (24) as described in (25-28). Differential equations were written for each species in the mechanisms described in Schemes 3 and 4 (see Results and Discussion), and the stopped-flow absorbance traces were directly fit by expressing the absorbance intensity ($D_c$) at any reaction time $t$ as the sum of the background absorbance ($D_b$) and the absorbances of each i$^{th}$ intermediate $D_i(t)$:

$$D_c = D_b + \sum_{i=0}^{n} D_i(t)$$

where $D_i(t) = \varepsilon_i[E_i(t)]$, $\varepsilon_i$ are the extinction coefficients at the specific wavelength for each discernible intermediate, and $[E_i(t)]$ are the concentrations of this intermediate at any given time $t$ ($i = 0$ relates to the free protein; $i > 0$ relates to the protein–inhibitor complexes).

In the data processing, global fits of sets of kinetic traces obtained at different concentrations of the reactants were done to derive the relevant kinetic scheme and to determine the kinetic parameters. In the fits all rate constants (including rate constants for the forward and backward reactions) as well as the specific molar extinction coefficients for all intermediate complexes were optimized.

*Steady state kinetics* – Inhibition of L-methionine γ-elimination reaction by L-cycloserine was determined in the reaction mixtures containing 100 mM potassium phosphate buffer (pH 8.0), 0.1 mM PLP, 1 mM EDTA, 5 mM DTT, and varied amounts of the substrate and the inhibitor. The rate of α-ketobutyrate accumulation was determined using dinitrophenylhydrazine (23). The reaction was initiated by addition of the enzyme (15 μg). The mixture was incubated for 15 min at 30°C, and the reaction was stopped by addition of trichloroacetic acid to the final concentration of 12.5% (w/v). Analysis of the data was processed by Dixon (29) and Lineweaver and Burk plots (30) and inhibition constant was determined using the EnzFitter program.

*Crystallization and data collection* – Crystals of MGL were obtained in the same conditions as described in (31) using polyethylene glycol monomethyl ether 2000 as the precipitant. The complex of MGL with L-cycloserine was obtained by soaking of holoenzyme crystals in cryoprotective mother liquid solution, containing L-cycloserine (50 mM, 7 min). The diffraction data were obtained at the BW6B DESY beamline with MAR345 MAResearch Image Plate. The detailed data collecting statistics are shown in Table 1.

*Structure determination and refinement* – The structure was solved by molecular replacement using the structure of *C. freundii* MGL (PDB ID 2RFV) by rigid body procedure, implemented in CCP4 software suite (32).

The model was improved using manual rebuilding with a COOT (33) and maximum likelihood refinement using REFMAC5 (34). Flexible loops of the protein and water molecules were removed from the initial model to exclude model bias during the first round of refinement. The presence of covalently bound to the PLP cycloserine molecule is clearly visible in the experimental *2Fo-Fc* and *Fo-Fc* electron density maps. The final model also contains a chloride ion, 266 water and 4 polyethylene glycol monomethyl ether 2000 molecules. The structure has been deposited to the Protein Data Bank with PDB ID 4OMA.

## RESULTS AND DISCUSSION

*Reaction of methionine γ-lyase with glycine* – It was shown that MGL catalyzes exchange of both Cα-protons of glycine with high stereospecificity

for (*pro*)-R-proton which reacts by a factor of 1440 faster than does *pro*-(S)-proton (35). In principle the exchange may proceed through the formation of a quinonoid intermediate, or by a concerted mechanism implying fast and reversible transfer of the (*pro*)-R-proton from Cα-atom to C4'-atom, or a formation of a six-membered transition state incorporating a water molecule (36) (Scheme 2). To assess the formation and decay of individual intermediates which are formed in the reaction of MGL with glycine, we carried out single-wavelength stopped-flow experiments at 320, 420 and 500 nm.

The time courses of absorbance at two single-wavelengths for the interaction of MGL with glycine are presented in Figure 1. Single-wavelength kinetic curves at 420 nm indicate that the reaction of glycine with MGL consists of two phases: fast (within a time interval of 20 ms) and slow (up to 100 s) increase of absorbance (Fig. 1A). On the other hand the absorbance at 320 nm is characterized by a fast increase for about 100 ms and a slow decrease till 100 s (Fig. 1B). The absorbance at 500 nm was stable over 200 s indicating very small level of formation of the quinonoid intermediate, which evidently is not the major intermediate.

During the global fitting of kinetic data a variety of kinetic models were examined, in order to ascertain the simplest kinetic mechanism that accurately described the experimental data at 420 nm and 320 nm simultaneously. Global fitting analysis showed that a reaction mechanism consisting of three steps and presented in Scheme 3 is the minimal one to appropriately describe the kinetic data. It should be noted that residuals (Supplementary Fig. S2) for both 320 nm and 420 nm have the same amplitude of deviation from the zero line in the whole range of time that gives us confidence on the reliability of the proposed kinetic mechanism. The rate and the equilibrium constants calculated using Scheme 3 are listed in Table 2. The steady state rate constant ($k_{ex}$) of the isotopic exchange of the two enantiotopic protons of glycine (35) are also presented in Table 2. Having compared the exchange rates with the other rates in Table 2 it was supposed that the complex $(E•Gly)_1$, which absorbs at 420 nm, and is formed in a millisecond time interval, probably corresponds to the external aldimine intermediate with orthogonal orientation of the "right" *pro*-(R)-proton ($H_r$) to the cofactor plane (IIIa). Such conformation is suitable for the exchange of namely this proton. On the other hand, complex $(E•Gly)_3$, which also absorbs at 420 nm, but is formed much slower, may correspond to the external aldimine in other conformation, with an orthogonal orientation of the 'wrong" *pro*-(S)-proton ($H_w$) (IIIb, Fig. 2). This conformation is suitable for the exchange of *pro*-(S)-proton, while exchange of the *pro*-(R)-proton is not possible. The observed rate of *pro*-(S)-proton exchange is slower than the rate of $(E•Gly)_3$ formation, so, in principle, this complex may be an intermediate in the isotopic exchange reaction.

In accordance with the proposed scheme the external aldimine is rearranged from conformation IIIa to conformation IIIb through the formation of an intermediate complex $(E•Gly)_2$, absorbing at 320 nm. Probably most possible structure of complex $(E•Gly)_2$ may be the ketimine, whose formation can be affected by abstraction of Cα-proton of the external aldimine and protonation of C4'-atom of the cofactor. In the reaction of MGL with its natural substrate such transformation is one of necessary catalytic stages (Scheme 1) (17). It seems possible also that the structures III, IIIa, IV, and V exist in a rapid equilibrium with each other. Alternatively complex $(E•Gly)_2$ may have a structure of the enolimine tautomer of the external aldimine (Scheme 2). Formation of such structure from the cationic external aldimine (IIIa) may be possible due to a conformational change of the protein, associated with an increase of hydrophobicity of the active site (37,38). Besides a conformer of the external aldimine with aldimine bond out of the plane of the cofactor and neutral form of the enolimine absorb in this region. This interpretation of the absorbance changes during binding of glycine is in agreement with the occurrence of fast Cα-proton exchange. According to crystal structure of the external aldimine of MGL with glycine (36) and known role of active site Lys residue as abstracting *pro*-(R)-proton in external aldimines of many PLP-dependent enzymes $(E•Gly)_1$ conformation fits with that having orthogonal *pro*-(R)-proton.

*Reactions of methionine γ-lyase with L-alanine and L-norvaline* – The kinetic traces are similar for L-alanine and L-norvaline (Fig. 3, 4). In both cases of interaction of MGL the latest possible intermediate is an enamine (See Supplementary Scheme S1). For these amino acids the existence of exchange of both Cα- and Cβ-protons was shown (19). Two discernable steps can be noticed on the absorbance traces. The first one is the

absorbance decay at 420 nm and the increase at 320 nm (up to 1 s), and the second one is a slow increase at 420 nm and slow decrease at 320 nm (up to 1000 s). The absorbance at 500 nm during interaction MGL with L-alanine and L-norvaline is slightly changed (data not shown) indicating that the quinonoid is a temporary intermediate and it is not accumulated in the reaction. The simplest mechanism that can account for the kinetic data is presented in Scheme 4, and includes the conversion of internal aldimine, absorbing at 420 nm, into complex (E•L-AA)1, which absorbs at 320 nm, and slow conversion of this complex into the external aldimine (E•L-AA)2, which absorbs at 420 nm. The calculated rate constants of the formation of the (E•L-AA)2 complex in the reactions with L-alanine and L-norvaline are much less than the rate constants of the isotopic exchange of Cα- and Cβ-protons in the both amino acids (Table 2). Consequently, the external aldimine (E•L-AA)2 cannot be an intermediate in the exchange reactions. It seems likely that in its structure (IIIc, Fig. 2) the side chain of the bound amino acid, but not the Cα-proton, is oriented orthogonally to the PLP, and the exchange of the Cα-proton is not possible. This structure formally is analogous to that of the slowly forming external aldimine (IIIb, Fig. 2) in the reaction with glycine, responsible for the exchange of the "wrong" *pro*-(S)-proton. Thus the isotopic exchange of both Cα- and Cβ-protons of L-alanine and L-norvaline should proceed through the intermediate complex (E•L-AA)1, absorbing at 320 nm. For the exchange of β-protons the formation of ketimine is strongly required (17), and we can reasonably suppose that the complex (E•L-AA)1 corresponds to the ketimine, existing in a fast equilibrium with the enolimine tautomer of the external aldimine also absorbing at 320 nm.

*Inhibition of γ-elimination reaction by L-cycloserine* – Cycloserine is a cyclic analogue of serine and D-cycloserine is known as natural antibiotic. L- and D-enantiomers of cycloserine are inhibitors of a number of PLP-dependent enzymes belonging to different classes. The γ-eliminating activity of MGL was reduced in the course of incubation with L-cycloserine. Inactivation by L-cycloserine was completely reversed by dialysis against potassium phosphate buffer (pH 8.0), containing 0.5 mM PLP and 5 mM DTT. *K*i value determined by EnzFitter was 0.068 mM. Linearization of the data in Lineweaver and Burk plot indicated inhibition of mixed type (Fig. 5A). It was shown that application of Dixon plots in conjunction with double reciprocal plots is useful for the identification of inhibition behavior (39). The experimental data were fitted to straight lines in Dixon plot (Fig. 5B) thus confirming mixed type of MGL inhibition by L-cycloserine. We were not able to observe any significant isotopic exchange of cycloserine protons, at least in conditions analogous to that in which the exchange had been observed with other inhibitors.

*X-ray structure of L-cycloserine–PLP-derivative* – Overall conformation of the polypeptide chains of MGL holoenzyme (PDB ID 2RFV) and MGL-cycloserine complex proved to be almost identical (RMSD for Cα-atoms of holoenzyme and the complex is 0.28 Å). There is the difference in the positions of two protein loops, N-terminal domain loop 45-60 and C-terminal domain loop 350-370, located nearby the active site. In the structures of the holoenzyme (PDB ID 2RFV and 1Y4I) the N-terminal loop is notably flexible. In the structure under consideration, in the structures of Michaelis complexes of MGL with a number of amino acids (20), and in the structure of external aldimine with glycine (36), it is stabilized. Most likely, the locking of the N-terminal domain loop provides optimal positioning of two cofactor-binding residues (Tyr58 and Arg60) and several active site hydrophobic pocket residues (Phe49, Leu57 and Leu61). At the same time in spatial structures of the complexes of the enzyme with amino acids, the C-terminal segment becomes more flexible. In the presented structure average B-factor of residues 350-370 (around 60 $Å^2$) increases as compared with average B-factor of the same residues (about 45 $Å^2$) in the holoenzyme structure (PDB ID 2RV). This flexibility may assist in a withdrawal of the products from the active site. We speculate that the N-terminal and the C-terminal segments make a "shutter" to ensure an access of a substrate to the active site, efficient catalysis, and a withdrawal of the products from the active site.

The resulting *2Fo-Fc* and *Fo-Fc* maps indicated the presence of cycloserine molecule covalently bound to PLP (Fig. 6). A well defined

region of electron density is connected to the cofactor and is clearly separated from any protein residues, including Nζ atom of Lys210, which forms covalent bond with PLP in the holoenzyme. We attempted to incorporate two tautomers of PLP-bound L-cycloserine into the electron density. One of them should possess planarity of the five-membered ring due to presence of double bond between C and N atoms of the cycloserine; the second does not have this restrain and could be bent. Comparison of the possible fitting of the two structures revealed better matching of the planar cycloserine to the experimental electron density.

The C3-C4-C4A-N dihedral angle is -5.1° and constrained by hydrogen bond between N and O3' atoms. The C4-C4A-N-CA dihedral angle is 167.4° and the C4A-N-CA-CB dihedral angle is -4.7° so the plane of the L-cycloserine is somewhat tilted with respect to the pyridine ring (Fig. 6). The geometry of the complex is corresponding to $sp^3$ hybridization of C4A which is implied by the shift of the band of MGL internal aldimine at 420 nm to 320 nm observed in polarized absorption spectra of holoenzyme crystal in the presence of L-cycloserine (40) and in absorption spectrum of the complex in a solution (data not shown). Accordingly, the N-CA bond of the complex should be double; the exocyclic oxygen atom connects to the cycloserine ring by single bond and is protonated. The structure corresponds to ketimine intermediate (Scheme 5) and matches well with that described for the complex of dialkylglycine decarboxylase with L-cycloserine (41).

The stereochemical position of the L-cycloserine-PLP complex in the active site is determined by firmly fixed contacts with amino acid residues of two subunits which are involved in the organization of a catalytic dimer. The endocyclic oxygen of the ring interacts with the hydrogen of NH group of main chain Ser339 from one side and with nearest water molecule from the other side (Fig. 7). The exocyclic oxygen makes hydrogen bonds with NH1 and NH2 atoms of Arg374. This residue is involved in a binding of carboxylic groups in the external aldimine of MGL with glycine (36) and in Michaelis complexes of the enzyme with some substrates and inhibitors (20). The position of the bound cycloserine is additionally stabilized by stacking with side chains of Tyr58 from the neighboring subunit and with Tyr113 of its own protein chain.

The coenzyme part of the complex is held in place by all the usual interactions observed in PLP-dependent enzymes. The phosphate is anchored by a number of polar interactions with the protein (14). The N1 atom of the pyridine ring forms H-bond with carboxylate of Asp185. O3' hydroxyl of PLP has no contacts with the protein atoms and is involved in hydrogen bonding with ketimine N atom of the complex (Fig. 7). In the structure there are tilts of PLP ring around the C5-C2 axis and Tyr113 ring to the solvent in comparison with their positions in the holoenzyme (25° and 19° respectively). Similar tilts of the cofactor (17°) and Tyr113 (28°) rings was demonstrated in three dimensional structure of external aldimine of the enzyme with glycine (36). Nε atom of Lys210 occupies two a little different positions close to ketimine N atom (~3.5Å). The abstraction of a Cβ-proton from the first ketimine intermediate is the next step of γ-elimination reaction. Data on crystal structure of *C. freundii* MGL external aldimine with glycine (36) allowed us to suppose that in the course of γ-elimination reaction 1,3-prototropic shift of Cα-proton to C4'-atom of the cofactor and the abstraction of a β-proton may proceed with the participation of Lys210. In the structure under consideration close positive charge of the ketimine N atom may stabilize the basic form of Lys210, which allows the stage of Cβ-proton abstraction to proceed. In both positions Nζ atom of Lys210 is close (3.75 Å, 3.15 Å) to Cβ-atom of cycloserine ring.

In 1959 several mechanisms were proposed for interaction of cycloserine with PLP-dependent enzymes including formation of stable isoxazole system and an opening of cycloserine ring with further transformations (42). Evidences for first mechanism were obtained in 1998 for γ-aminobutyric acid aminotransferase (43) and for D-amino acid aminotransferase (44). It was proposed that an abstraction of a β-proton of cycloserine from ketimine by active site lysine residue leads to stable aromatic cycloserine-PLP complex. At the resolution of our structure we do not exclude a saturation of N-CA bond but the geometry of the complex is more compatible with double N-CA bond. For mechanisms of γ-elimination and γ-replacement reactions catalyzed by PLP-dependent enzymes it was postulated that ketimine (Scheme 1, V) is plausible intermediate for effective labilization of Cβ-proton to proceed (17). Its formation in the course of these reactions catalyzed by *E. coli* cystathionine γ-synthase was

detected by stopped-flow data in the same paper. The evidence of ketimine intermediate was obtained by X-ray data for cystathionine γ-synthase (45).

*Reaction of methionine γ-lyase with L-cycloserine* – In steady-state absorption spectrum of MGL complexed with L-cycloserine the band belonging to the internal aldimine with maximum in the region 420 nm disappeared along with the appearance the predominant band at the region 320-330 nm (data not shown).

The reaction of MGL with L-cycloserine leads to a single change of absorbance within 2000 s: a decrease at 420 nm and an increase at 320 nm, the rates of the two processes being identical (Fig. 8). According to X-ray data the possible intermediate of the reaction of MGL with L-cycloserine is ketimine, which has absorbance maximum at the region of 320 nm. It can be assumed that the observed spectral changes correspond to the decomposition of external aldimine and accumulation of ketimine, respectively (Scheme 5). The external aldimine is converted to a ketimine intermediate without detectable changes at 500 nm, indicating that the intermediate quinonoid species are not accumulating in the reaction.

The processing of the L-cycloserine by MGL was described by kinetic Scheme 4. The values for individual kinetic constants were determined by global fitting (Table 2). (E•L-AA)1 complex more likely corresponds to external aldimine, which subsequently transforms in ketimine in the complex (E•L-AA)2 (Scheme 5). Interestingly, the forward rate constant $k_1$ and $k_2$ are similar to the respective constants for L-norvaline reaction. At the same time the reverse rate constant $k_{-1}$ and $k_{-2}$ are 58 and 1.6 times less as compared to L-norvaline reaction, indicating that MGL complexes with L-cycloserine are more stable, which leads to shift of the equilibrium to the ketimine intermediate.

The stability of ketimine intermediate may explain the higher inhibition of the reaction with L-methionine in comparison with glycine, L-alanine and L-norvaline. The *K*i value of inhibition of γ-elimination of L-methionine by L-cycloserine is at least tenfold less that the *K*i values for glycine, L-alanine and L-norvaline (Table 2).

## CONCLUSION

The comparison of values of the rate constants characterizing the processes of the amino acids bindings by MGL showed that the equilibrium constant of the first step $K_1 = k_1/k_{-1}$ is increased in the row: glycine < L-norvaline ~ L-alanine < L-cycloserine. The rate constant of the forward reaction $k_1$ for glycine, L-norvaline and L-cycloserine is in the range of $(1.0\text{-}4.0)\times10^4$ $M^{-1}s^{-1}$, being at least 10 times higher than in the case of L-alanine (Table 2). Interestingly, the rate constant of the isotopic exchange of Cα-protons for L-alanine is 10 times smaller than that of glycine and L-norvaline (19). The process characterized with the rate constant $k_1$ should represent the complex mechanism including not only multistage process of the Schiff base formation between incoming amino acid and Lys210, but possibly the enzyme reorganization during the incorporation of the amino acid into the active site. The rate constant $k_{-1}$, which characterizes the decomposition of the first complex (Table 2), reflects the stability of this state. In cases of L-alanine and L-cycloserine the magnitude of $k_{-1}$ is more than 150 and 50 times lower than the same value for glycine and L-norvaline.

Formation of the "right" external aldimine enables the formation of the ketimine intermediate which was obviously registered in the cases of L-norvaline and L-alanine and probably for glycine ([E•L-Nva]1, [E•L-Ala]1 or ([E•Gly]2 complexes, respectively). The last detected complex (([E•L-Nva]2, [E•L-Ala]2 or ([E•Gly]3) likely corresponds to the external aldimine in the "wrong" conformation. In the case of L-cycloserine the formation of (E•L-cSer)1 complex reflects the formation of the external aldimine. The subsequent transformations (abstraction of Cα-proton and protonation of C4'-atom of PLP) lead to accumulation of stable ketimine intermediate.

The kinetic data have shown that amino acids incorporate in the active site of MGL in the proper conformation owing to the conformational selectivity of the active site. The Schiff bases can be formed with an amino acid only having "right" orientation of the side chain, Cα-hydrogen and carboxyl group relatively to PLP plane. After the formation of the ketimine intermediate the flat structure of amino acid can be turned in the active site of enzyme thus after the reversible protonation the amino acid would be in the "wrong" conformation (e.g. IIIb, Fig. 2).

In general, both X-ray and kinetic analyses of the interaction of MGL with L-cycloserine provide the direct proof of ketimine intermediate formation

in the catalytic mechanism of PLP-dependent γ-elimination reaction.

## REFERENCES


1. El-Sayed, A. S. (2010) Microbial L-methioninase: production, molecular characterization, and therapeutic applications. *Appl. Microbiol. Biotechnol.* **86**, 445-467
2. Manukhov, I. V., Mamaeva, D. V., Rastorguev, S. M., Faleev, N. G., Morozova, E. A., Demidkina, T. V., and Zavilgelsky, G. B. (2005) A gene encoding L-methionine gamma-lyase is present in *Enterobacteriaceae* family genomes: identification and characterization of *Citrobacter freundii* L-methionine gamma-lyase. *J. Bacteriol.* **187**, 3889-3893
3. Ito, S., Nakamura, T., and Eguchi, Y. (1976) Purification and characterization of methioninase from *Pseudomonas putida*. *J. Biochem.* **79**, 1263-1272
4. Nakayama, T., Esaki, N., Lee, W. J., Tanaka, I., Tanaka, H., and Soda, K. (1984) Purification and Properties of L-Methionine Gamma-Lyase from *Aeromonas Sp*. *Agric. Biol. Chem.* **48**, 2367-2369
5. Kreis, W., and Hession, C. (1973) Isolation and purification of L-methionine-alpha-deamino-gamma-mercaptomethane-lyase (L-methioninase) from *Clostridium sporogenes*. *Cancer Res.* **33**, 1862-1865
6. Yoshimura, M., Nakano, Y., Yamashita, Y., Oho, T., Saito, T., and Koga, T. (2000) Formation of methyl mercaptan from L-methionine by *Porphyromonas gingivalis*. *Infect. Immun.* **68**, 6912-6916
7. Fukamachi, H., Nakano, Y., Okano, S., Shibata, Y., Abiko, Y., and Yamashita, Y. (2005) High production of methyl mercaptan by L-methionine-alpha-deamino-gamma-mercaptomethane lyase from *Treponema denticola*. *Biochem. Biophys. Res. Commun.* **331**, 127-131
8. Tokoro, M., Asai, T., Kobayashi, S., Takeuchi, T., and Nozaki, T. (2003) Identification and characterization of two isoenzymes of methionine gamma-lyase from *Entamoeba histolytica*: a key enzyme of sulfur-amino acid degradation in an anaerobic parasitic protist that lacks forward and reverse trans-sulfuration pathways. *J. Biol. Chem.* **278**, 42717-42727
9. Lockwood, B. C., and Coombs, G. H. (1991) Purification and characterization of methionine gamma-lyase from *Trichomonas vaginalis*. *Biochem. J.* **279 ( Pt 3)**, 675-682
10. Rebeille, F., Jabrin, S., Bligny, R., Loizeau, K., Gambonnet, B., Van Wilder, V., Douce, R., and Ravanel, S. (2006) Methionine catabolism in *Arabidopsis cells* is initiated by a gamma-cleavage process and leads to S-methylcysteine and isoleucine syntheses. *Proc. Natl. Acad. Sci. U.S.A.* **103**, 15687-15692
11. Hoffman, R. M. (1997) Methioninase: a therapeutic for diseases related to altered methionine metabolism and transmethylation: cancer, heart disease, obesity, aging, and Parkinson's disease. *Human cell* **10**, 69-80
12. Sato, D., and Nozaki, T. (2009) Methionine gamma-lyase: the unique reaction mechanism, physiological roles, and therapeutic applications against infectious diseases and cancers. *IUBMB life* **61**, 1019-1028
13. Tan, Y., Xu, M., and Hoffman, R. M. (2010) Broad selective efficacy of recombinant methioninase and polyethylene glycol-modified recombinant methioninase on cancer cells *In Vitro*. *Anticancer Res.* **30**, 1041-1046
14. Nikulin, A., Revtovich, S., Morozova, E., Nevskaya, N., Nikonov, S., Garber, M., and Demidkina, T. (2008) High-resolution structure of methionine gamma-lyase from *Citrobacter freundii*. *Acta Crystallogr. D Biol. Crystallogr.* **64**, 211-218
15. Tanaka, H., Esaki, N., and Soda, K. (1985) A versatile bacterial enzyme: L-methionine gamma-lyase. *Enz. Microbiol. Technol.* **7**, 530-537
16. Tanaka, H., Esaki, N., and Soda, K. (1977) Properties of L-methionine gamma-lyase from *Pseudomonas ovalis*. *Biochemistry* **16**, 100-106
17. Brzovic, P., Holbrook, E. L., Greene, R. C., and Dunn, M. F. (1990) Reaction mechanism of *Escherichia coli* cystathionine gamma-synthase: direct evidence for a pyridoxamine derivative of

vinylglyoxylate as a key intermediate in pyridoxal phosphate dependent gamma-elimination and gamma-replacement reactions. *Biochemistry* **29**, 442-451

18. Davis, L., and Metzler, D. E. (1971) Pyridoxal-linked elimination and replacement reactions. *Adv. Enzymol.* **35**, 33-74
19. Morozova, E. A., Bazhulina, N. P., Anufrieva, N. V., Mamaeva, D. V., Tkachev, Y. V., Streltsov, S. A., Timofeev, V. P., Faleev, N. G., and Demidkina, T. V. (2010) Kinetic and spectral parameters of interaction of *Citrobacter freundii* methionine gamma-lyase with amino acids. *Biochemistry (Mosc).* **75**, 1272-1280
20. Revtovich, S. V., Morozova, E. A., Khurs, E. N., Zakomirdina, L. N., Nikulin, A. D., Demidkina, T. V., and Khomutov, R. M. (2011) Three-dimensional structures of noncovalent complexes of *Citrobacter freundii* methionine gamma-lyase with substrates. *Biochemistry (Mosc).* **76**, 564-570
21. Kudou, D., Misaki, S., Yamashita, M., Tamura, T., Takakura, T., Yoshioka, T., Yagi, S., Hoffman, R. M., Takimoto, A., Esaki, N., and Inagaki, K. (2007) Structure of the antitumour enzyme L-methionine gamma-lyase from *Pseudomonas putida* at 1.8 A resolution. *J. Biochem.* **141**, 535-544
22. Lowry, O. H., Rosebrough, N. J., Farr, A. L., and Randall, R. J. (1951) Protein measurement with the Folin phenol reagent. *J. Biol. Chem.* **193**, 265-275
23. Friedemann, T. E., and Haugen, G. E. (1943) Pyruvic acid, the determination of keto acids in blood and urine. *J. Biol. Chem.* **147**, 415-443
24. Kuzmic, P. (1996) Program DYNAFIT for the analysis of enzyme kinetic data: application to HIV proteinase. *Anal. Biochem.* **237**, 260-273
25. Kuznetsov, N. A., Zharkov, D. O., Koval, V. V., Buckle, M., and Fedorova, O. S. (2009) Reversible Chemical Step and Rate-Limiting Enzyme Regeneration in the Reaction Catalyzed by Formamidopyrimidine-DNA Glycosylase. *Biochemistry* **48**, 11335-11343
26. Koval, V. V., Kuznetsov, N. A., Ishchenko, A. A., Saparbaev, M. K., and Fedorova, O. S. (2010) Real-time studies of conformational dynamics of the repair enzyme *E. coli* formamidopyrimidine-DNA glycosylase and its DNA complexes during catalytic cycle. *Mutat. Res.* **685**, 3-10
27. Kuznetsov, N. A., Koval, V. V., Zharkov, D. O., and Fedorova, O. S. (2012) Conformational dynamics of the interaction of *Escherichia coli* endonuclease VIII with DNA substrates. *DNA Repair (Amst)* **11**, 884-891
28. Kuznetsov, N. A., Vorobjev, Y. N., Krasnoperov, L. N., and Fedorova, O. S. (2012) Thermodynamics of the multi-stage DNA lesion recognition and repair by formamidopyrimidine-DNA glycosylase using pyrrolocytosine fluorescence--stopped-flow pre-steady-state kinetics. *Nucleic Acids Res.* **40**, 7384-7392
29. Dixon, M. (1953) The determination of enzyme inhibitor constants. *Biochem. J.* **55**, 170-171
30. Lineweaver, H., and Burk, D. (1934) The determination of enzyme dissociation constants. *J. Am. Chem. Soc.* **56**, 658-566
31. Mamaeva, D. V., Morozova, E. A., Nikulin, A. D., Revtovich, S. V., Nikonov, S. V., Garber, M. B., and Demidkina, T. V. (2005) Structure of *Citrobacter freundii* L-methionine gamma-lyase. *Acta Crystallogr. Sect. F Struct. Biol. Cryst. Commun.* **61**, 546-549
32. Winn, M. D., Ballard, C. C., Cowtan, K. D., Dodson, E. J., Emsley, P., Evans, P. R., Keegan, R. M., Krissinel, E. B., Leslie, A. G., McCoy, A., McNicholas, S. J., Murshudov, G. N., Pannu, N. S., Potterton, E. A., Powell, H. R., Read, R. J., Vagin, A., and Wilson, K. S. (2011) Overview of the CCP4 suite and current developments. *Acta Crystallogr. D Biol. Crystallogr.* **67**, 235-242
33. Emsley, P., Lohkamp, B., Scott, W. G., and Cowtan, K. (2010) Features and development of Coot. *Acta Crystallogr. D Biol. Crystallogr.* **66**, 486-501
34. Murshudov, G. N., Skubak, P., Lebedev, A. A., Pannu, N. S., Steiner, R. A., Nicholls, R. A., Winn, M. D., Long, F., and Vagin, A. A. (2011) REFMAC5 for the refinement of macromolecular crystal structures. *Acta Crystallogr. D Biol. Crystallogr.* **67**, 355-367

35. Koulikova, V. V., Zakomirdina, L. N., Gogoleva, O. I., Tsvetikova, M. A., Morozova, E. A., Komissarov, V. V., Tkachev, Y. V., Timofeev, V. P., Demidkina, T. V., and Faleev, N. G. (2011) Stereospecificity of isotopic exchange of C-alpha-protons of glycine catalyzed by three PLP-dependent lyases: the unusual case of tyrosine phenol-lyase. *Amino acids* **41**, 1247-1256
36. Revtovich, S. V., Faleev, N. G., Morozova, E. A., Anufrieva, N. V., Nikulin, A. D., and Demidkina, T. V. (2014) Crystal structure of the external aldimine of *Citrobacter freundii* methionine gamma-lyase with glycine provides insight in mechanisms of two stages of physiological reaction and isotope exchange of alpha- and beta-protons of competitive inhibitors. *Biochimie* **101**, 161-167
37. Johnson, G. F., Tu, J. I., Bartlett, M. L., and Graves, D. J. (1970) Physical-chemical studies on the pyridoxal phosphate binding site in sodium borohydride-reduced and native phosphorylase. *J. Biol. Chem.* **245**, 5560-5568
38. Shaltiel, S., and Cortijo, M. (1970) The mode of binding of pyridoxal 5'-phosphate in glycogen phosphorylase. *Biochem. Biophys. Res. Commun.* **41**, 594-600
39. Butterworth, P. J. (1972) The use of Dixon plots to study enzyme inhibition. *Biochim. Biophys. Acta* **289**, 251-253
40. Ronda, L., Bazhulina, N. P., Morozova, E. A., Revtovich, S. V., Chekhov, V. O., Nikulin, A. D., Demidkina, T. V., and Mozzarelli, A. (2011) Exploring methionine gamma-lyase structure-function relationship via microspectrophotometry and X-ray crystallography. *Biochim. Biophys. Acta* **1814**, 834-842
41. Malashkevich, V. N., Strop, P., Keller, J. W., Jansonius, J. N., and Toney, M. D. (1999) Crystal structures of dialkylglycine decarboxylase inhibitor complexes. *J. Mol. Biol.* **294**, 193-200
42. Kochetkov, N. K., Khomutov, R. M., Karpeisky, M. Y., Bydovsky, E. I., and Severin, E. S. (1959) The mechanism of antibiotic action of cycloserine. *Doklady Akademii Nayk SSSR* **129**, 1132-1134
43. Olson, G. T., Fu, M. M., Lau, S., Rinehart, K. L., and Silverman, R. B. (1998) An aromatization mechanism of inactivation of gamma-aminobutyric acid aminotransferase for the antibiotic L-cycloserine. *J. Am. Chem. Soc.* **120**, 2256-2267
44. Peisach, D., Chipman, D. M., Van Ophem, P. W., Manning, J. M., and Ringe, D. (1998) D-cycloserine inactivation of D-amino acid aminotransferase leads to a stable noncovalent protein complex with an aromatic cycloserine-PLP derivative. *J. Am. Chem. Soc.* **120**, 2268-2274
45. Steegborn, C., Laber, B., Messerschmidt, A., Huber, R., and Clausen, T. (2001) Crystal structures of cystathionine gamma-synthase inhibitor complexes rationalize the increased affinity of a novel inhibitor. *J. Mol. Biol.* **311**, 789-801

## FOOTNOTES

[*]This work was supported by the Program of the Russian Academy of Sciences "Molecular & Cell Biology" (6.11); Russian Foundation for Basic Researches (14-04-00349), the Grant from Russian Scientific Foundation (14-14-00063), the grants of the President of the Russian Federation for state support of the leading scientific schools (SS-2064.2014.4, SS-1205.2014.4), Russian Ministry of Education and Science (SP-4012.2013.4).

[§]To whom correspondence should be addressed. T.V.D. Tel.: +7(499)135 9858, Email: tvd@eimb.ru; O.S.F. Tel: +7(383)363 5174; Email: fedorova@niboch.nsc.ru

[1]Institute of Chemical Biology and Fundamental Medicine, Siberian Branch of the Russian Academy of Sciences, Novosibirsk 630090, Russia
[2]Department of Natural Sciences, Novosibirsk State University, Novosibirsk 630090, Russia
[3]Nesmeyanov Institute of Organoelement Compounds, Russian Academy of Sciences, Moscow 119991, Russia
[4]Engelhardt Institute of Molecular Biology, Russian Academy of Sciences, Moscow 119991, Russia
[5]Institute of Protein Research, Russian Academy of Sciences, Pushchino, Moscow Region, 142290, Russia
[6]The abbreviations used are: MGL, methionine γ-lyase; PLP, pyridoxal 5'-phosphate; L-cSer, L-cycloserine; L-Nva, L-norvaline; PDB, Protein Data Bank.

**SCHEMES AND FIGURES LEGENDS**

**Scheme 1.** Chemical mechanism of the γ-elimination reaction.

**Scheme 2.** The possible intermediates in the reaction of glycine with MGL.

**Scheme 3.** Kinetic mechanism of MGL interaction with glycine.

**Scheme 4.** Kinetic mechanism of MGL processing of L-alanine, L-norvaline and L-cycloserine.

**Scheme 5.** The possible intermediates in the reaction of L-cycloserine with MGL.

**FIGURE 1. Interaction of MGL and glycine as monitored by changes of absorbance of the holoenzyme.** Time courses were recorded at pH 7.8, 0.1 M potassium phosphate buffer solution, containing 0.5 mM DTT and 0.1 mM EDTA, with the concentration of MGL fixed at 12.5 μM. Time courses were obtained at 25 °C. Solution of enzyme was mixed with various concentrations of glycine (10-500 mM). Each kinetic curve was averaged over at least four independent experiments. The absorbance at 420 nm (**A**) and 320 nm (**B**) was detected. Solid lines represent the fitted curves.

**FIGURE 2. Schematic representation of possible aldimine conformers of amino acids in the active site of MGL.**

**FIGURE 3. Interaction of MGL and L-alanine as monitored by changes of absorbance of the holoenzyme.** Time courses were recorded at pH 7.8, 0.1 M potassium phosphate buffer solution, containing 0.5 mM DTT and 0.1 mM EDTA, with the concentration of MGL fixed at 12.5 μM. Time courses were obtained at 25 °C. Solution of enzyme was mixed with various concentrations of L-alanine (1.0-12.0 mM). Each kinetic curve was averaged over at least four independent experiments. The absorbance at 420 nm (**A**) and 320 nm (**B**) was detected. Solid lines represent the fitted curves.

**FIGURE 4. Interaction of MGL and L-norvaline as monitored by changes of absorbance of the holoenzyme.** Time courses were recorded at pH 7.8, 0.1 M potassium phosphate buffer solution, containing 0.5 mM DTT and 0.1 mM EDTA, with the concentration of MGL fixed at 12.5 μM. Time courses were obtained at 25 °C. Solution of enzyme was mixed with various concentrations of L-norvaline (1.5-7.5 mM). Each kinetic curve was averaged over at least four independent experiments. The absorbance at 420 nm (**A**) and 320 nm (**B**) was detected. Solid lines represent the fitted curves.

**FIGURE 5. The inhibition of the γ-elimination reaction by L-cycloserine.** Lineweaver and Burk (**A**) and Dixon (**B**) plots.

**FIGURE 6. Stereo view of PLP-cycloserine derivative with the final *2Fo – Fc* map contoured at the 1.5 σ level.**

**FIGURE 7. Stereo view of the active site.** H-bonds are indicated by green dashed lines. The shown distances are in Å.

**FIGURE 8. Interaction of MGL and L-cycloserine as monitored by changes of absorbance of the holoenzyme.** Time courses were recorded at pH 7.8, 0.1 M potassium phosphate buffer solution, containing 0.5 mM DTT and 0.1 mM EDTA, with the concentration of MGL fixed at 12.5 μM. Time courses were obtained at 25 °C. Solution of enzyme was mixed with various concentrations of L-cycloserine (6.35-38.1 μM). Each kinetic curve was averaged over at least three independent experiments. The absorbance at 420 nm (**A**) and 320 nm (**B**) was detected. Solid lines represent the fitted curves.

## TABLES

**Table 1.** Data collection and refinement statistics. Values in parentheses are for the highest resolution shell.

| | |
|---|---|
| Space group | *I222* |
| Unit cell parameters (Å) | $a$ = 56.27, $b$ = 122.89, $c$ = 126.61, α=β=γ=90 |
| Wavelength (Å) | 0.843 |
| Resolution (Å) | 15-1.60 (1.65-1.60) |
| No. of unique reflections | 55080 |
| Mean I/σ(I) | 17.3 (3.6) |
| Completeness (%) | 94.5 (94.3) |
| Redundancy | 4.5 (3.9) |
| $R_{sym}$ (%) | 4.8 (39.6) |
| *Refinement* | |
| Resolution range (Å) | 15-1.6 (1.64-1.60) |
| Rwork | 0.139 (0.197) |
| Rfree | 0.275 (0.293) |
| No. of protein atoms | 2993 |
| No. of water atoms | 266 |
| No. of heterogenic atoms | 57 |
| Mean temperature factor $B$ (Å$^2$) | 28.69 |
| R.m.s. deviation from ideal values | |
| Bond lengths (Å) | 0.019 |
| Bond angles (°) | 1.985 |
| Ramachandran plot | |
| Favoured region (%) | 97.11 |
| Allowed region (%) | 2.10 |
| Outlier region (%) | 0.79 |

**Table 2.** Pre-steady-state and isotopic exchange kinetic parameters for interaction of MGL (from *Citrobacter freundii)* with amino acids.

| Constants* | Glycine | L-alanine | L-norvaline | L-cycloserine |
|---|---|---|---|---|
| $k_1$, $M^{-1}s^{-1}$ | $(1.0 \pm 0.2)\times10^{4}$ | $(7.0 \pm 0.1)\times10^{2}$ | $(4.0 \pm 1.0)\times10^{4}$ | $(3.6 \pm 1.2)\times10^{4}$ |
| $k_{-1}$, $s^{-1}$ | $140 \pm 30$ | $0.6 \pm 0.1$ | $94.0 \pm 6.0$ | $1.6 \pm 0.3$ |
| $k_2$, $s^{-1}$ | $1.5 \pm 0.1$ | $(6.8 \pm 0.5)\times10^{-3}$ | $(6.6 \pm 0.4)\times10^{-3}$ | $(6.5 \pm 2.5)\times10^{-3}$ |
| $k_{-2}$, $s^{-1}$ | $33.5 \pm 1.3$ | $(3.6 \pm 0.4)\times10^{-3}$ | $(6.3 \pm 0.2)\times10^{-3}$ | $(3.8 \pm 0.4)\times10^{-4}$ |
| $k_3$, $s^{-1}$ | $0.3 \pm 0.1$ | - | - | |
| $k_{-3}$, $s^{-1}$ | $0.08 \pm 0.04$ | - | - | |
| $K_1$, mM | 14 | 0.9 | 2.3 | 0.045 |
| $K_2$ | 22.3 | 0.53 | 1.0 | 0.58 |
| $K_3$ | 0.27 | | | |
| *K*i, mM | 49** | 3.4** | 4.7** | 0.068±0.07 |
| $k_{ex}^{\alpha\text{-H}}$, $s^{-1}$ *** | 20.2 *pro*-(R)<br>$1.4\times10^{-3}$ *pro*-(S) | 2.71 | 20.6 | - |
| $k_{ex}^{\beta\text{-H}}$, $s^{-1}$ *** | - | 2.63 | 11.1 | - |

* $K\text{n} = k_{-n}/k_n$

** *K*i for glycine, L-alanine and L-norvaline from (19).

*** $k_{ex}$ for glycine from (35), L-alanine and L-norvaline from (19).

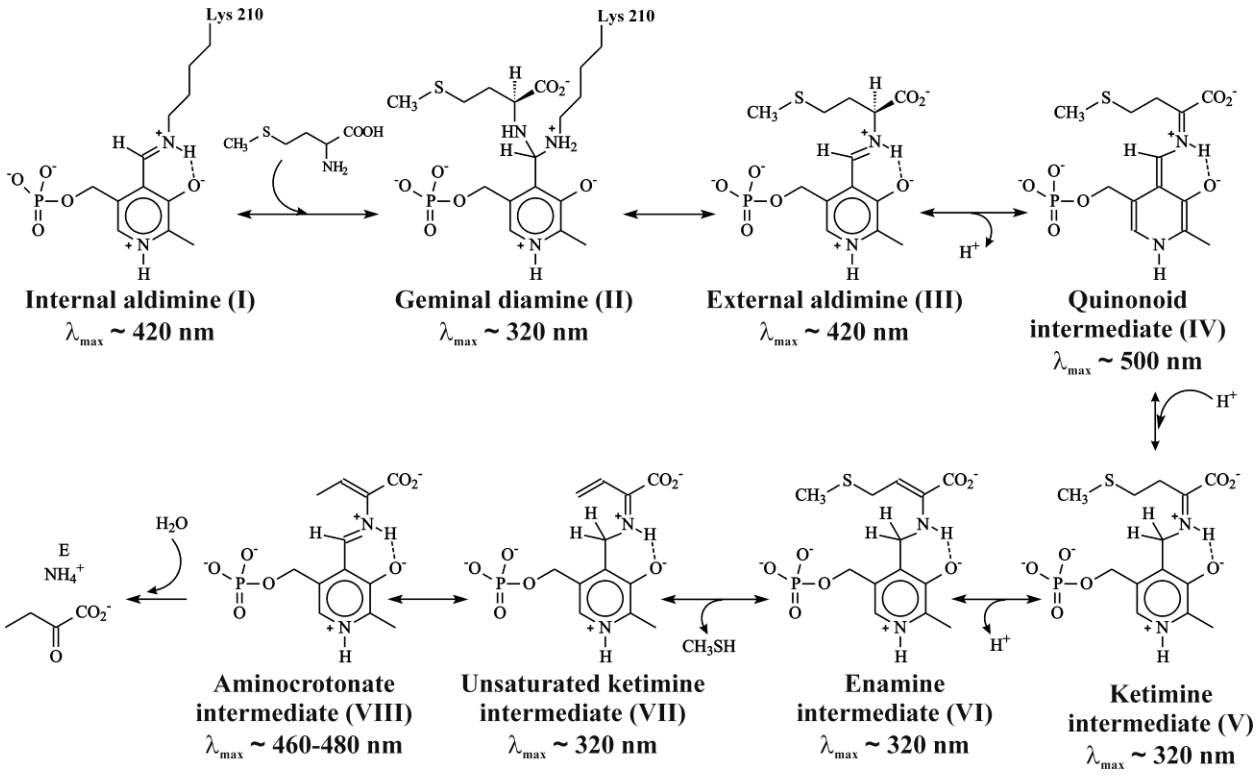


**Scheme 1.** (2-column width)

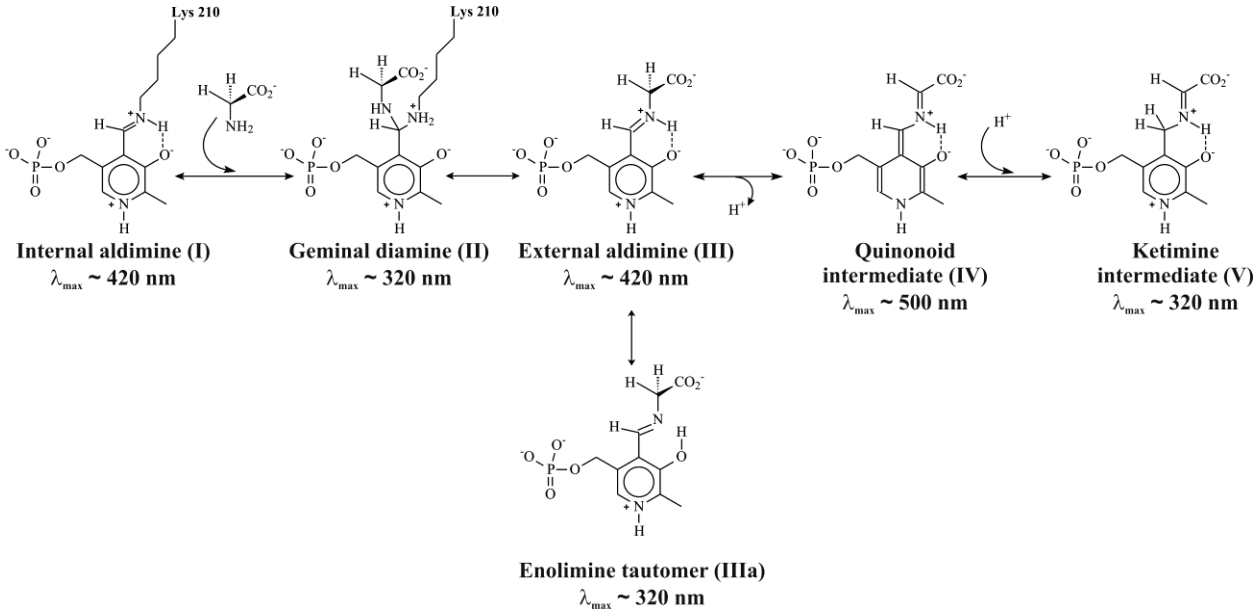


**Scheme 2.** (2-column width)

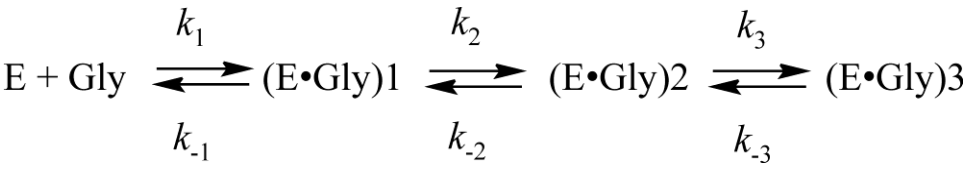


**Scheme 3.** (1.5-column width)

$$\text{E + L-AA} \underset{k_{-1}}{\overset{k_1}{\rightleftharpoons}} \text{(E•L-AA)1} \underset{k_{-2}}{\overset{k_2}{\rightleftharpoons}} \text{(E•L-AA)2}$$

**Scheme 4.** (1-column width)

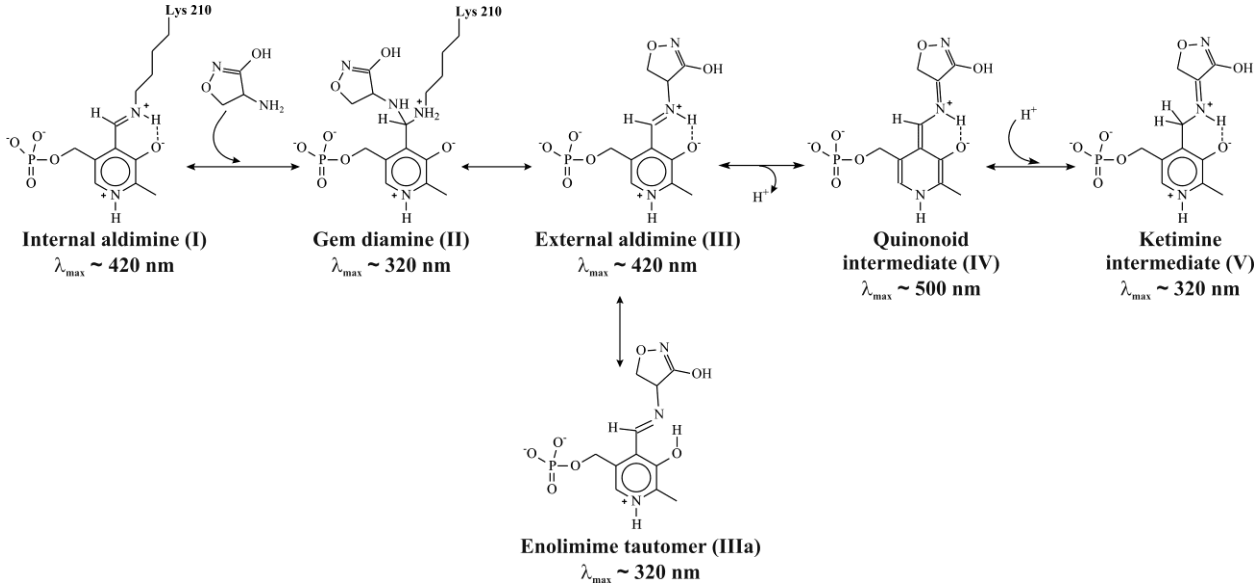


**Scheme 5.** (2-column width)

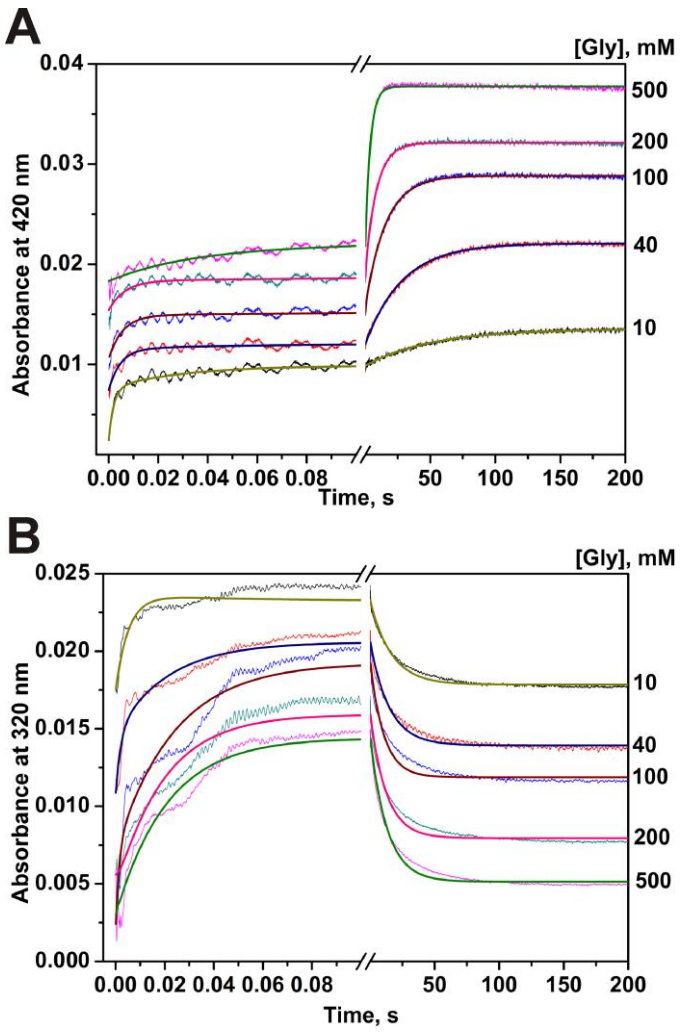


Figure 1.
(1-column width)

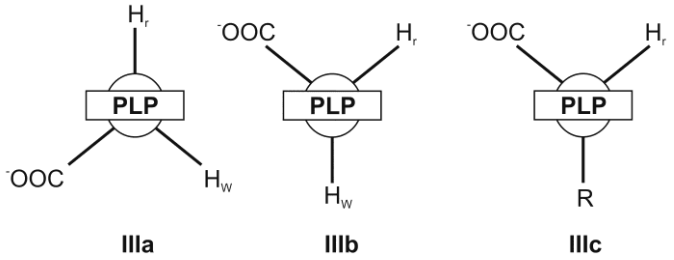


Figure 2.
(1-column width)

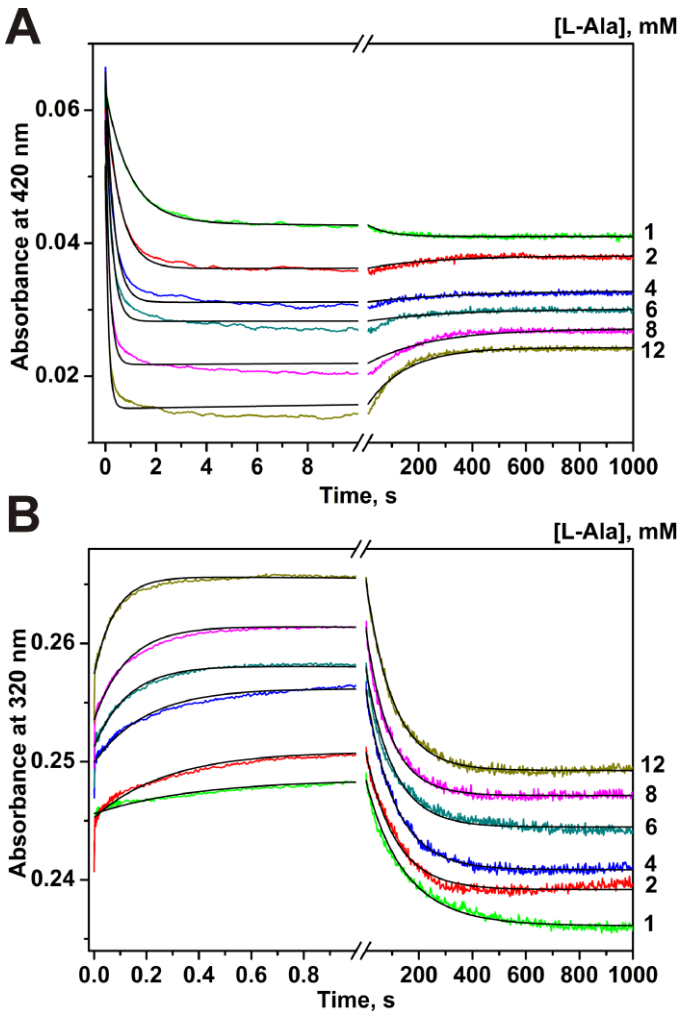


Figure 3.
(1-column width)

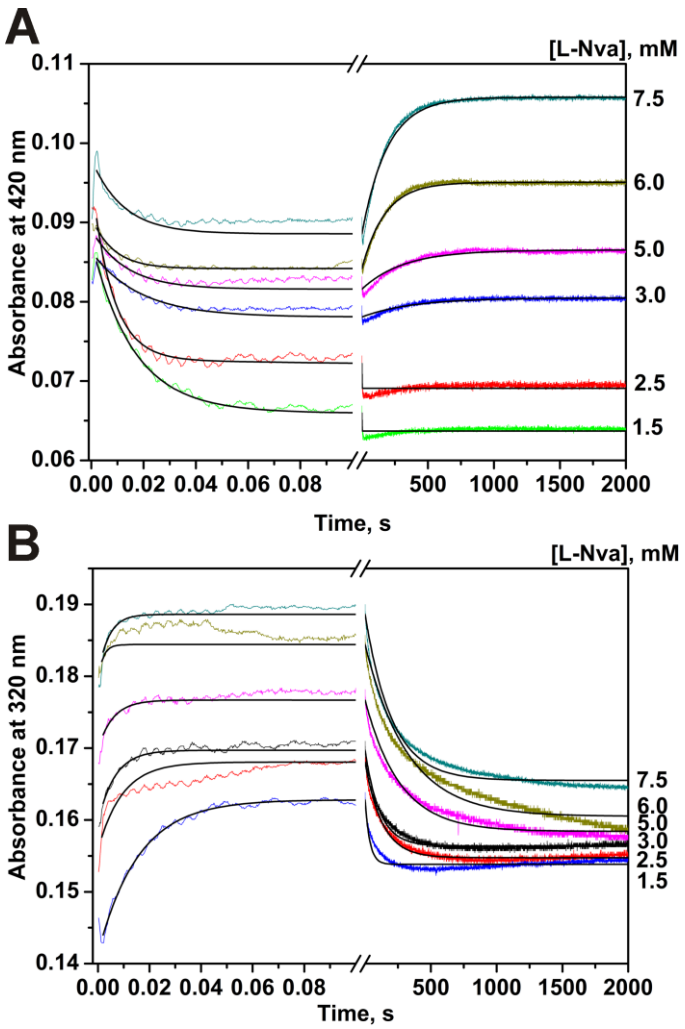


Figure 4.
(1-column width)

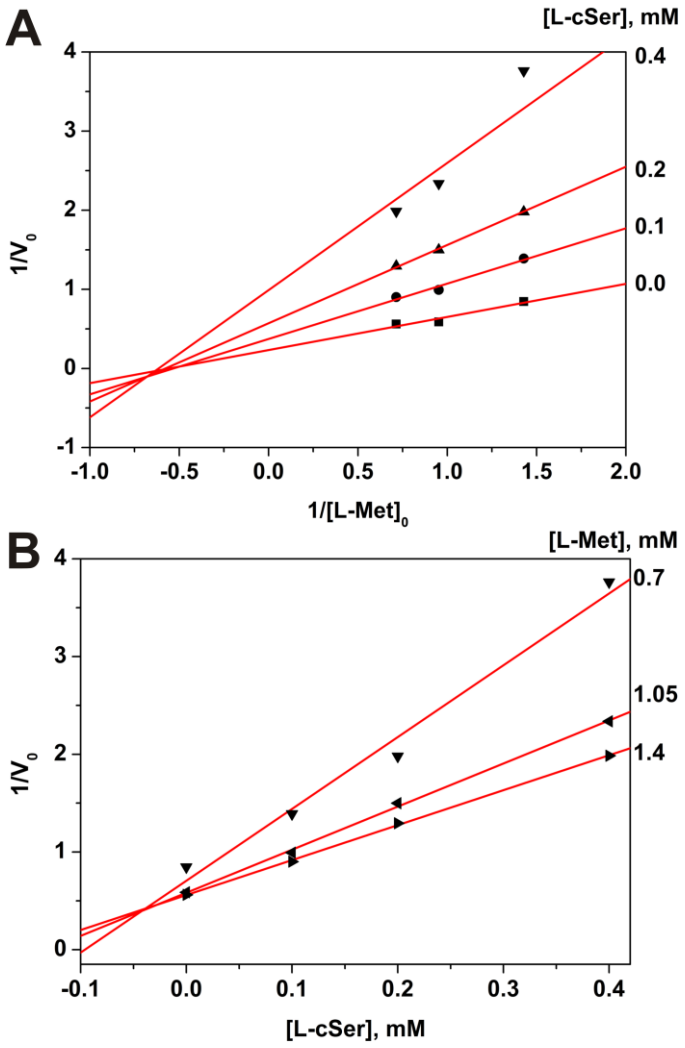


Figure 5.
(1-column width)

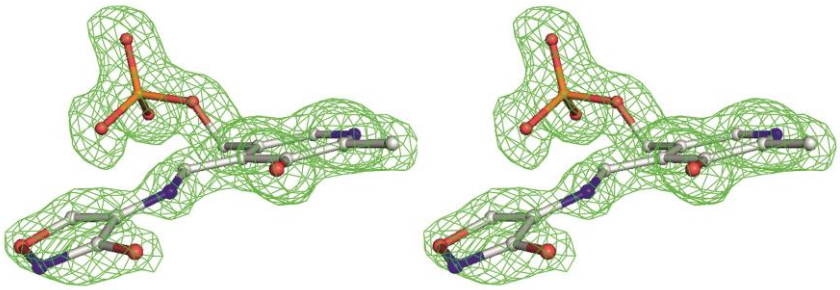

Figure 6.
(1.5-column width)

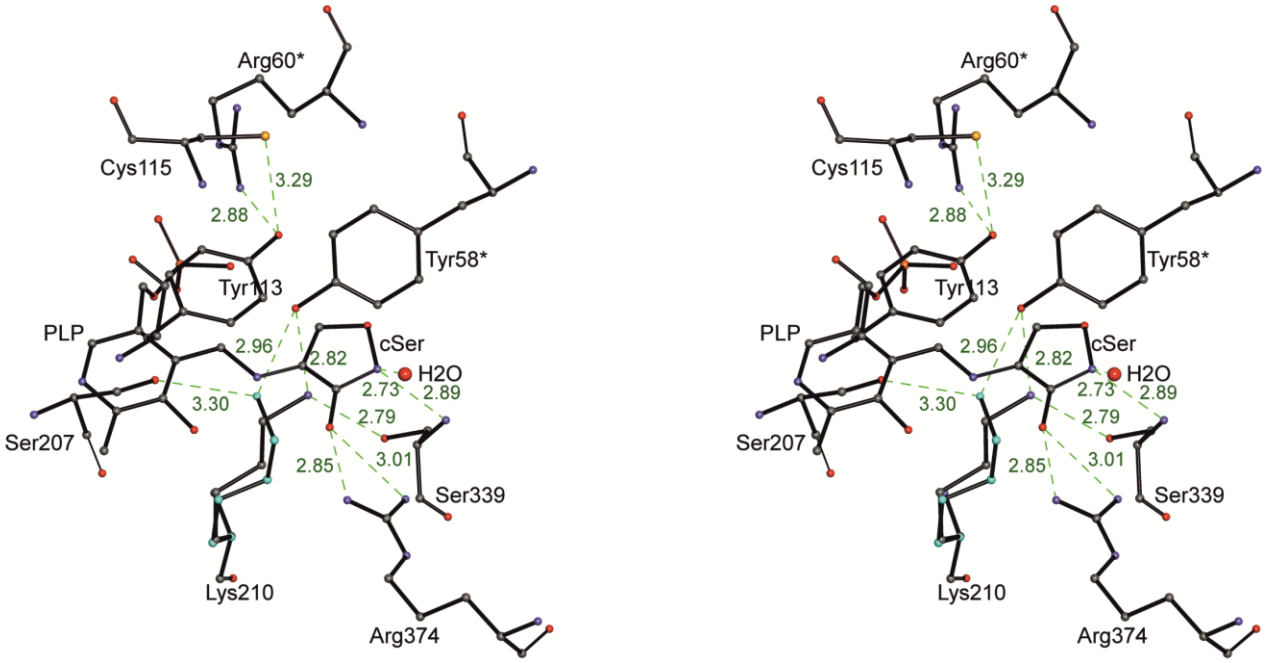


Figure 7.
(2-column width)

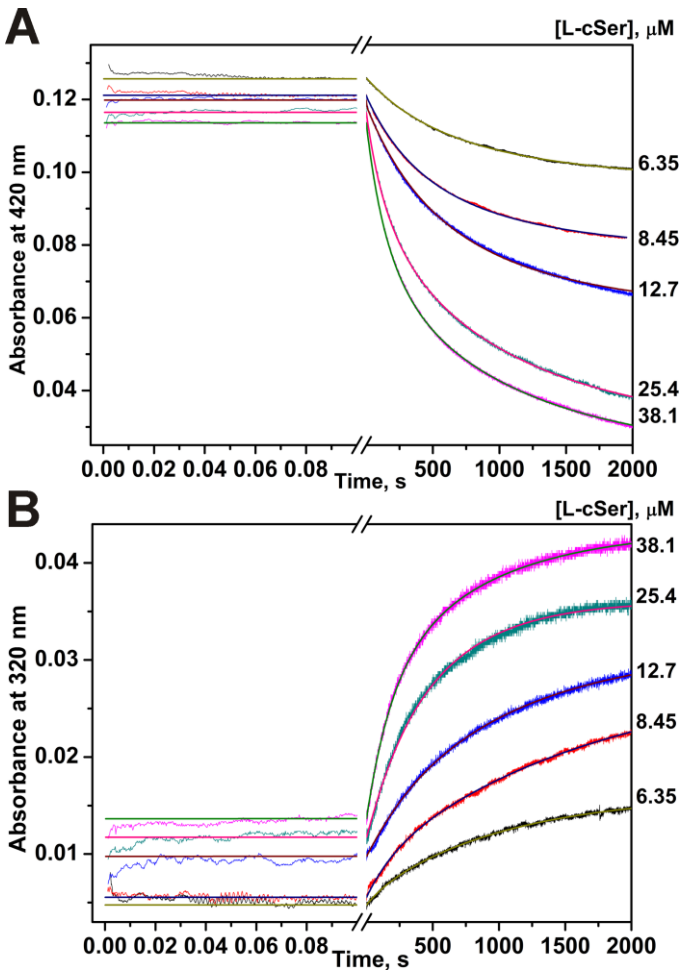


Figure 8.
(1-column width)